Microcontamination 94 Conference Proceedings, October 4-6, 1994, San Jose, California, p. 39-48

PARTICLE TRANSPORT IN PLASMA REACTORS

Daniel J. Rader, Sandia National Laboratories; Anthony S. Geller, Sandia National Laboratories; Seung J. Choi, Sandia National Laboratories; and Mark J. Kushner, University of Illinois.

INTRODUCTION

SEMATECH and the Department of Energy have established a Contamination Free Manufacturing Research Center (CFMRC) located at Sandia National Laboratories. One of the programs underway at the CFMRC is directed towards defect reduction in semiconductor process reactors by the application of computational modeling. The goal is to use fluid, thermal, plasma, and particle transport models to identify process conditions and tool designs that reduce the deposition rate of particles on wafers. The program is directed toward defect reduction in specific manufacturing tools, although some model development is undertaken when needed. The need to produce quantifiable improvements in tool defect performance requires the close cooperation among Sandia, universities, SEMATECH, SEMATECH member companies, and equipment manufacturers. Currently, both plasma (*e.g.,* etch, PECVD) and nonplasma tools (*e.g.,* LPCVD, rinse tanks) are being worked on under this program.

In this paper, we summarize our recent efforts to reduce particle deposition on wafers during plasma-based semiconductor manufacturing. Although particle transport in specific processing tools is being studied, this paper will instead focus on particle transport in a generic, parallel-plate reactor geometry that is applicable to a range of single wafer process tools. In plasma tools, both process parameters (*e.g.,* pressure, flow rate, rf power, and geometry) and particle parameters (*e.g.,* size and density) control particle transport within the reactor and must be considered. Particle concentrations are assumed to be low enough to allow a dilute approximation, for which the coupling between the fluid/plasma and particle phases is one-way. In this case, the fluid/thermal/plasma transport equations can be solved either analytically or numerically neglecting the particle phase; the resulting velocity, temperature, electric, and ion flux fields are then used as input for the particle transport calculations. Particle diffusion is neglected at present. Order of magnitude calculations suggest that diffusion will not generally influence trap locations, although diffusion could lead to trap broadening. Temperature, fluid, and particle transport (in the absence of plasma) have been modeled using both commercial and specialized codes. For particle transport in plasma, the program has relied heavily on 2-D plasma models developed at the University of Illinois [1]. Although the results presented here represent continuum transport calculations, work is now underway to predict particle transport in noncontinuum flow using Discrete Simulation Monte Carlo (DSMC) techniques developed at Sandia National Laboratories [2]. One-way coupling is again assumed, so that the DSMC calculations are performed neglecting particle effects, and particle trajectories are calculated in a post-processing mode using the DSMC results.

During its passage through a plasma tool, a wafer is exposed to a variety of environments, including the plasma process step as well as wafer handling (*e.g.,* loadlock entry and exit, venting, purging) and tool preparation (*e.g.,* flow or pressure equalization) steps. Thus, particle reduction in plasma tools requires that particle deposition under both plasma and neutral-flow conditions be considered. When the plasma is on, particle transport is characterized by the well-known appearance of particle "traps" first reported by Roth and Spears [3]. Presumably, particles

DISCLAIMER

Portions of this document may be illegible in electronic image products. Images are produced from the best available original document.

accumulate at regions within the plasma where the forces acting on them are in balance; typically the traps are fairly stable (although complex) structures which have been studied experimentally by many authors in a variety of plasma discharges [4-13]. The traps can appear in a variety of shapes (planar, conical, domes, rings, *etc.*); typically, large particles are found near the sheath edge, while small particles accumulate towards the center of the discharge at the location of the maximum in the plasma potential. Material topography and composition have been shown experimentally to influence trap formation [8,12,13]. Experimental evidence also supports the widely accepted belief that particles suspended in a plasma gain a negative charge [4,14]; more recently, calculations [15-18] have also shown that particles acquire a substantial negative charge.

In the absence of plasma, the forces contributing to particle transport in plasma tools include neutral fluid viscous drag, gravity, thermophoresis, and electrostatic (if the particle is charged and electric fields are present in the reactor). In the presence of plasma, Sommerer *et al.* [19] and Barnes *et al.* [20] have proposed that electrostatic and viscous ion drag forces must also be considered. Acting alone, the electrostatic force would accelerate negatively charged particles towards the center of electropositive plasmas or towards local maxima in the plasma potential. Acting alone, the ion drag force would tend to accelerate particles in the direction of net ion flux (typically towards reactor boundaries). The transport or trapping of particles in a plasma is the resultant of all of the above forces; several investigators have shown that thermophoresis, fluid drag, or gravity can strongly influence particle transport under some plasma conditions [11,21].

A key question in defect reduction is determining when particles deposit on the wafer, since this helps identify the transport mechanisms controlling deposition. Environmental transients associated with loadlock operation, wafer handling, and process chamber preparation steps are widely considered to add defects. Analysis of these non-plasma sources requires sophisticated (and computationally expensive) transient models for neutral flow. In some cases, the problem can be simplified by considering steady state flow but a transient particle generation event. This approach is reasonable when characteristic times for the fluid or plasma fields to reach steady state are much smaller than the characteristic times associated with particle transport; this quasi-steady approximation has been assumed in all of our work to date. Although particles have been widely observed trapped in plasmas, there is current debate as to the mechanism by which these particles move to the wafer. If the traps are strong enough to hold all of the particles, then deposition during the actual plasma step would be expected to be small. However, recent calculations by Choi *et al.* have shown that 1 μm diameter particles become more likely to escape the trap as RF power is increased [22]. Another path is that the particles deposit after the plasma is extinguished. Experimental work reported by Jellum *et al.* showed that the particles remaining in the interelectrode gap after the plasma was extinguished were uncharged [11]. In this case, particle transport to the wafer would be controlled by non-plasma forces (neutral fluid drag, gravity, thermophoresis) and the significance of trap-prediction would be in determining particle initial positions. Note that all of these observations are likely to depend on specific plasma process conditions (chemistry, pressure, power, *etc.*) and chamber geometry.

Next, we review the dominant forces acting on a particle in a plasma reactor. Other forces (*e.g.* photophoresis or shear lift) are generally expected to be small compared to those listed, but they could become important in some specific applications. We then describe model predictions for trap locations, and particle deposition after the plasma is extinguished. Also, the results have been used to develop a list of general guidelines that should help in the design of inherently-clean plasma reactors.

PARTICLE FORCES

The free molecule limit is given in the following force expressions which only applies in the limit of very large particle Knudsen number; this is a good assumption for the low pressures typical of plasma processes (< 1 Torr) and the small particle sizes of interest (< 1 μm diameter).

Electrostatic

The electrostatic force acting on a particle of charge Q_p in an electric field $\boldsymbol{E}$ is:

$$\boldsymbol{F}_E = Q_p \boldsymbol{E} \,. \tag{1}$$

The form of Equation (1) is deceptively simple. With or without a plasma, a determination of either the particle charge or the local electric field can be a challenging task. For particles suspended in plasma, there has been significant progress in predicting particle charge using orbital motion limited (OML) analytic [16,17] or Particle-in-Cell (PIC) computational [18] techniques. The PIC and OML results are in good agreement. Based on the PIC calculations, the charge on a particle in a plasma can be approximated as:

$$Q_p \approx -800 d_p T_e e \tag{2}$$

where d_p is the particle diameter (in μm here), T_e is the electron temperature (in eV here), and e is the electronic charge. For example, a 1 μm particle in a plasma with an electron temperature of 2 eV would carry a charge of about $-1600e$. Note that Equation (2) assumes that the particles are few in number (a good assumption for plasma etch processes). For PECVD systems where particle concentrations can be high, see Choi and Kushner [18]. In calculating the net electrostatic force, the full (unshielded) particle charge - Equation (2) - is combined with calculations or measurements of the local electric field $\boldsymbol{E}$ in the absence of particles [17].

Viscous Ion Drag

The ion drag force is caused by momentum exchange between positively charged ions as they drift past the negatively charged particles. Momentum can be transferred either by direct collisions or by electrostatic interactions. Again, there has been significant progress in predicting ion drag using OML analytic [16,17] or PIC computational [18] techniques. As with particle charge, the PIC and OML results are in good agreement. The determination of the ion drag force requires an integration over the ion velocity distribution function, and the reader is referred to the literature for the details [16,17,18]. Generally, the result of the ion drag force in an electropositive plasma is to push particles toward the electrodes; electrode topography and materials can modify this result locally.

Neutral Viscous Drag

The drag on a particle in neutral molecular flow is [23]:

$$F_D = \frac{1}{3}\left(1 + \frac{\pi\alpha}{8}\right)\pi\rho c d_p^2 (V_g - V_p) \tag{3}$$

where d_p is the particle diameter, ρ is the gas mass density, $c=(8kT/\pi m)^{1/2}$ is the mean thermal velocity of the gas, V_g and V_p are the gas and particle velocity, and α is the accommodation coefficient representing the fraction of gas molecules undergoing diffuse reflection at the particle surface (the remainder undergo specular reflection). Typically, the value of α ranges between 0.8 and 0.9 for most gas-particle combinations.

Thermophoresis
The neutral thermophoretic force acting on a particle in the free molecule limit is:

$$F_T = -\frac{8}{15} d_p^2 \frac{\lambda_{tran}}{c} \nabla T \tag{4}$$

where λ_{tran} is the translational part of the thermal conductivity for the gas, and ∇T is the gas phase temperature gradient [24].

Gravity
The force of gravity acting on a particle is:

$$F_G = m_p g = \frac{\pi}{6} \rho_p d_p^3 g \tag{5}$$

where ρ_p is the particle material density and g is the gravitational acceleration.

Simplified View
A schematic diagram of how the various forces can interact in a parallel plate, showerhead-type single wafer plasma reactor is shown in Figure 1. The schematic shows the case of a heated lower electrode, which acts to repel particles. In cases where the lower electrode (and hence the wafer) are cooled relative to the rest of the chamber, the thermophoretic force would be directed toward the lower electrode and thus enhance deposition. Note that in the absence of any other forces (and in this simple geometry), the plasma-induced electrostatic and ion drag forces act in opposition and could result in the planar particle traps observed near the plasma sheath boundaries at each electrode. The exact position (or existence) of these traps depends on the interplay of the plasma-induced forces with gravity, thermophoresis, and fluid drag.

In this simple geometry little 2-D structure would be expected. However, real reactors have a number of features that could lead to the complex trapping structures observed experimentally: complex topography, material discontinuities, nonuniform flow, nonuniform electrode temperature, *etc.*

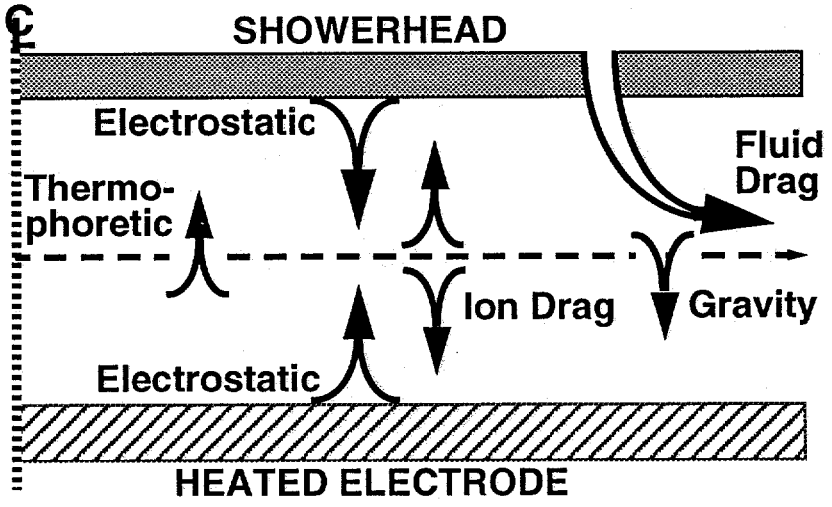

Figure 1. Schematic diagram of the forces acting on particles in a parallel-plate, showerhead-type plasma reactor. A heated electrode is assumed for thermophoresis.

PREDICTION OF PARTICLE TRAPS

To predict the position of particle traps, the neutral and plasma fields must first be calculated. For particle transport in plasma, the program has relied heavily on 2-D fluid and plasma models developed at the University of Illinois [1]. These models are used to calculate the local electric fields and ion flux within the plasma, which are needed to calculate the electrostatic and ion drag forces. Using these techniques, trap positions within a simple parallel plate, showerhead-type RF plasma have been calculated as a function of particle size, neutral flowrate, and RF power [22]. The results of some of these calculations for argon gas at 100 mTorr are reproduced in Figure 2.

As seen in Figure 2a, at low power a single planar trap is found located near the midplane of the reactor. As power is increased, the single trap separates into two traps which move towards the nearest electrode as RF power is increased. This is the result of the increase of ion drag relative to the electrostatic force. The change from one centered to two distinct traps with increasing RF power has recently been observed experimentally [25]. Figure 2b shows the effect of increasing gas flowrate at a fixed RF power. At low flowrates the two traps are clearly visible, but for flowrates above 100 sccm the neutral drag overcomes ion drag and the trap near the upper electrode disappears. This result clearly shows how neutral drag can overcome the plasma-induced forces on a particle under some conditions.

POST-PLASMA DEPOSITION

If the traps are strong enough to hold all of the particles, then deposition during the actual plasma step would be expected to be small. One explanation for defects in this case is that the particles deposit after the plasma is extinguished. In this section, we assume the particles remaining in the interelectrode gap after the plasma is extinguished are uncharged [11]. In this case, particle transport to the wafer would be controlled by non-plasma forces (neutral fluid drag, gravity, thermophoresis) and the significance of trap-prediction would be in determining particle initial positions. For simplicity we assume a showerhead-type, parallel plate reactor such as shown in Figure 1. We assume that the flow is isothermal and enters through the showerhead with a constant velocity; furthermore, we consider the case where the axial fluid velocity is independent of radius, and the radial velocity scales with radius (for elaboration of the assumptions see Rader *et al.* [26]). Under these assumptions, a similarity solution can be used which greatly reduces the computation of the flow field [27]. For the present analysis, particle inertia and diffusion have been neglected, although the current particle transport models do include these phenomena.

Based on these assumptions, Rader *et al.* [26] have analyzed the transport of a particle starting at axial position z_o and radial position r_o, where the local axial fluid velocity is $u(z_o)$. The following result gives the radial location, L, at which the particle deposits on the wafer:

$$\left(\frac{r_o}{L}\right)^2 = \frac{V_p^t}{u(z_o) + V_p^t} \tag{6}$$

where $V_p{}^t$ is the net particle drift velocity (velocity at which the drag force balances the applied forces acting to accelerate a particle). For example, if only gravity is present, $V_p{}^t$ is the terminal or settling velocity of the particle. Note that Equation (6) was arrived at considering the details of the assumed flowfield [26]; the same result can be found from analysis of the general result that, if diffusion and inertia are neglected, the deposition rate is independent of the flowfield for forces described by a potential [28].

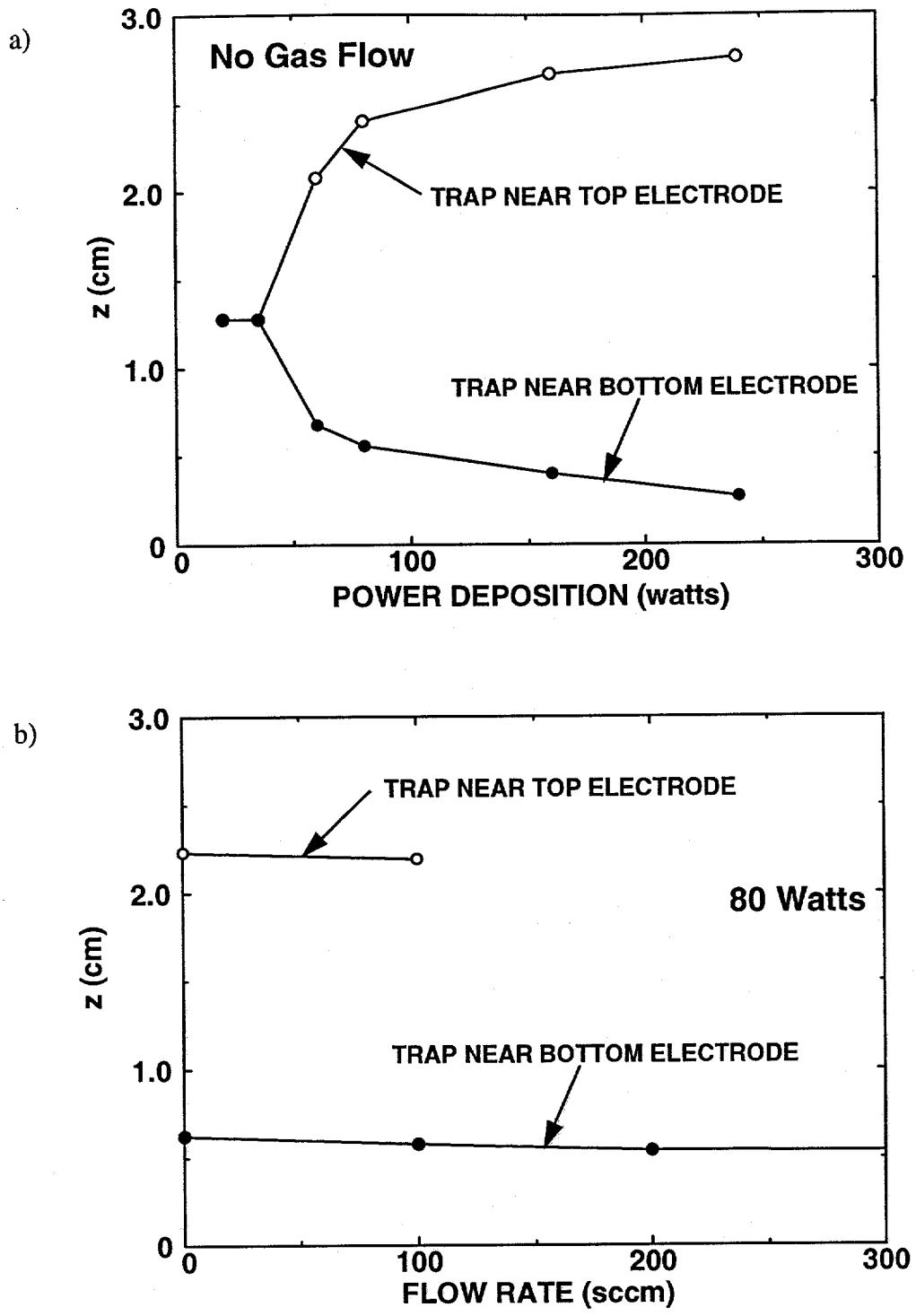

Figure 2. Dust particle trap locations in a parallel plate plasma reactor for a 100 mTorr argon plasma with a 3 cm gap: a) trap position vs. power for a one micron particle, b) trap position vs. flow rate for a one micron particle with 80 W power deposition. (a showerhead-type upper electrode is assumed at z=3 cm, with the wafer sitting on the lower electrode at z=0 cm; chamber diameter is 20 cm).

There are several interesting implications of Equation (6). First, consider particles entering a parallel-plate reactor with a uniform distribution across a showerhead of the same radius as the wafer, R_w. A collection efficiency, η, is defined as the fraction of particles entering the reactor through the showerhead which deposit on the wafer. An efficiency of one indicates that all particles end up on the wafer, while an efficiency of zero indicates that all particles exit the reactor with the flow. Equation (6) can be used to show that [26]:

$$\eta = \left(\frac{R_o}{R_w}\right)^2 = \frac{V_p^t}{U_o + V_p^t}. \tag{7}$$

where U_o is the fluid velocity at the showerhead and R_o gives the starting location of a particle traveling on a critical trajectory, *i.e.*, a particle that deposits exactly at the outer edge of the wafer. Particles originating closer to the centerline than R_o will deposit on the wafer, while particles originating farther from the centerline will exit with the flow. While Equation (7) gives a simple formula for estimating particle deposition on the wafer, it also shows that the particles depositing on the wafer tend to come from the central portion of the flow.

Equation (6), however, can also be used to predict particle deposition onto the wafer for particles originating anywhere within the reactor. A common example would be in predicting the deposition efficiency from particles released from a plasma-induced trap. For simplicity, assume that the particles are distributed uniformly in a horizontal trap at an axial position z_o. After the plasma is extinguished (and assuming the particles rapidly lose their charge), the fraction of particles in the trap that deposit on the wafer is given by:

$$\eta(z_o) = \left(\frac{R_o}{R_w}\right)^2 = \frac{V_p^t}{u(z_o) + V_p^t}. \tag{8}$$

where $u(z_o)$ is the local fluid velocity at the particle starting position z_o. Neither of the above equations depends on flow Reynolds number; *i.e.*, the derived efficiency expressions are valid for any laminar flow where the axial velocity profile is 1-D (also stagnation point flow [28]).

As an example, we consider a flow of 100 sccm argon gas in a parallel-plate reactor at a process pressure of 100 mTorr. The gap between the showerhead and wafer is assumed to be 4 cm, the wafer temperature is 293K, and the showerhead temperature is 333K. A linear temperature profile is assumed between the plates (giving a temperature gradient of 10 K/cm). Only gravity and thermophoresis are considered; both forces are assumed to be aligned normal to the wafer, and the terminal velocity contribution from each force is directed toward the wafer (positive in sign). Although each terminal velocity should be position dependent in practice (because of the temperature variations in the reactor), we assume both to be constant with the value calculated at the wafer temperature. The wafer and showerhead are assumed to be 200 mm in diameter, giving a gas velocity at the showerhead of 40.3 cm/s. A particle density of 1 g/cc is assumed.

Under these assumptions, the particle deposition efficiency for particles entering through the showerhead can be calculated using Equation (7); the calculated efficiency is plotted as a function of particle diameter in Figure 3 where the curve is labeled "showerhead." The efficiency below about 0.1 μm is flat as the thermophoretic velocity is nearly independent of particle size in this regime. For larger sizes, gravity becomes important and the efficiency increases. A second

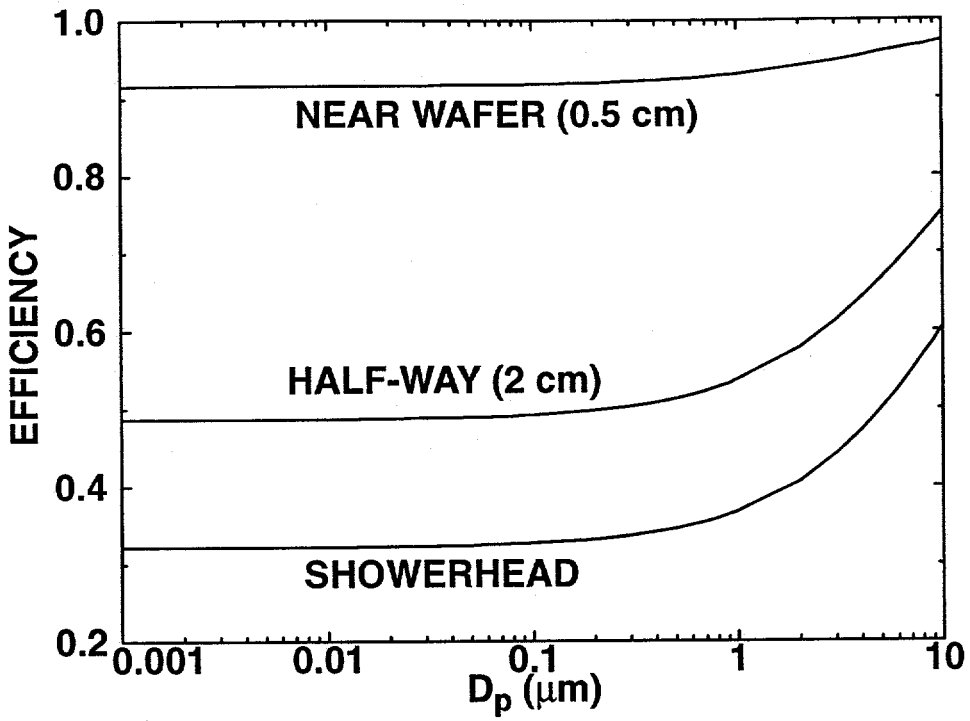

Figure 3. Collection efficiency as a function of particle size and starting position. Particles originating from the showerhead and two plasma-trap locations are shown: "half-way" indicates particles starting near the midplane of the reactor (2cm from the lower electrode), and "near wafer" indicates particles starting 0.5 cm from the wafer.

example is considered with the same process conditions but for the case of a plasma having concentrated the particles in traps located at different distances from the wafer. For this case, Equation (8) is used to produce the two efficiency curves labeled "half-way" and "near showerhead" in Figure 3. As shown, the effects of traps is to greatly increase particle deposition on the wafer when the traps force the particles nearer the wafer.

These results are consistent with industry experience which is that plasma shut-down at the end of the plasma process step must be carefully controlled. For example, lowering the RF power or the process pressure at the end of the process have been suggested as ways to move the particle traps farther from the wafer. However, the net effect on deposition can be complicated by the fact that some of these process changes (such as lowering the process pressure) may also increase the post-plasma deposition rate by increasing the drift velocity (see Equation (8)).

CONCLUSIONS

In defect reduction in plasma reactors, particle transport and deposition must be considered both in the presence and absence of plasma. Although particle trapping behavior in the presence of plasma is well known, the majority of particle deposition likely results during the nonplasma steps if the traps are strong. We have presented a simple analysis of how particle trap formation can greatly increase particle deposition efficiencies by moving the particles to starting positions nearer the wafer. This result suggests the importance of many of the controlled plasma shut-down strategies used in industry to reduce defects, and shows the interaction between the plasma and non-plasma process steps in determining ultimate defect levels.

Acknowledgments - This work was performed at Sandia National Laboratories under U.S. Department of Energy contract DE-AC04-94AL85000, and supported by the Contamination Free Manufacturing Research Center jointly operated by Sandia National Laboratories and SEMATECH. The authors thank Nadeem Alvi, Gene Feit, Randy Williams, and Venu Menon of SEMATECH; Scott Sibbett of SEMATECH and Intel; Dave Graves of UC Berkeley; and Don Schlosser of Lam Research who have greatly assisted us in this work.

REFERENCES

1. P.L.G. Ventzek, T.J. Sommerer, R.J. Hoekstra, and M.J. Kushner, *Appl. Phys. Lett. 63:* 605 (1993).

2. T.J. Bartel, C.R. Justiz, "DSMC simulation of ionized rarefied flows," *AIAA 93-3095,* AIAA 24th Fluid Dynamics Conference, Orlando, FL (1993)

3. R.M. Roth, K.G. Spears, G.D. Stein, and G. Wong, "Spatial dependence of particle light scattering in an RF silane discharge," *Appl. Phys. Lett. 46:* 253-255 (1985).

4. G.S. Selwyn, J. Singh, and R.S. Bennett "*In situ* laser diagnostic studies of plasma-generated particulate contamination," *J. Vac. Sci. Technol. A7(4):* 2758-2765. (1989).

5. J.A. Durham;, J.L. Petrucci, Jr., and Ch. Steinbruchel (1990) "Observing effects of source material, plasma chemistry, process parameters, and RF frequency on plasma-generated particles," *Microcontamination 8(11):* 37-39, 67-68 (1990).

6. G.M. Jellum and D.B. Graves, "Particulates in aluminum sputtering discharges," *J. Appl. Phys. 67:* 6490-6496 (1990).

7. G.M. Jellum and D.B. Graves, "Particle-plasma interaction in low-pressure discharges," *Appl. Phys. Lett. 57:* 2077-2079 (1990).

8. G.S. Selwyn, J.E. Heidenreich, and K.L. Haller, "Particle trapping phenomena in radio frequency plasmas," *Appl. Phys. Lett. 57:* 1876-1878 (1990).

9. Y. Watanabe, M. Shiratani, and H. Makino, "Powder-free plasma chemical vapor deposition of hydrogenated amorphous silicon with high RF power density using modulated RF discharge," *Appl. Phys. Lett. 57:* 1616-1618 (1990).

10. R.N. Carlile, S. Geha, J.F. O'Hanlon, and J.C. Stewart, "Electrostatic trapping of contamination particles in a process plasma environment," *Appl. Phys. Lett. 59:* 1167-1169 (1991).

11. G.M. Jellum, J.E. Daugherty, and D.B. Graves, "Particle thermophoresis in low pressure glow discharges," *J. Appl. Phys. 69:* 6923-6934 (1991).

12. G.S. Selwyn, J.E. Heidenreich, and K.L. Haller, "Rastered laser light scattering studies during plasma processing: Particle contamination trapping phenomena," *J. Vac. Sci. Technol. A9(5):* 2817-2824. (1991)

13. S.G. Geha, R.N. Carlile, J.F. O'Hanlon, and G.S. Selwyn, "The dependence of contamination particle traps on wafer material and topography," *J. Appl. Phys. 72:* 374-383 (1992)

14. J.J. Wu and R.J. Miller, *J. Appl. Phys. 67:* 1051 (1990).

15. R.N. Nowlin and R.N. Carlile, "The electrostatic nature of contaminative particles in a semiconductor processing plasma," *J. Vac. Sci. Technol. A9(5):* 2825-2833 (1991).

16. J.E. Daugherty, R.K. Porteous, M.D. Kilgore, and D.B. Graves, "Sheath structure around particles in low-pressure discharges," *J. Appl. Phys. 72:* 3934-3942 (1992).

17. J.E. Daugherty, R.K. Porteous, and D.B. Graves, "Electrostatic forces on small particles in low-pressure discharges," *J. Appl. Phys. 73:* 1617-1620 (1993).

18. S.J. Choi and M.J. Kushner, "A particle-in-cell simulation of dust charging and shielding in low pressure glow discharges," *IEEE Trans. Plasma Sci. 22(2):* 138-150 (1994).

19. T.J. Sommerer, M.S. Barnes, J.H. Keller, M.J. McCaughey, and M.J. Kushner, "Monte Carlo-fluid hybrid model of the accumulation of dust particles at sheath edges in radio-frequency discharges," *Appl. Phys. Lett. 59:* 638-640 (1991).

20. M.S. Barnes, J.H. Keller, J.C. Forster, J.A. O'Neill, and D.K. Coultas, "Transport of dust particles in glow-discharge plasmas," *Phys. Rev. Lett. 68:* 313-316 (1992).

21. J.F. O'Hanlon and J. Kang, "The behavior of particle clouds near vertically oriented wafers in a capacitively coupled RF discharge," *Proc. IES 40th Ann. Tech. Meeting,* 303-307 (1994).

22. S.J. Choi, P.L.G. Ventzek, R.J. Hoekstra, and M.J. Kushner, "Spatial distributions of dust particles in plasmas generated by capacitively coupled radio frequency discharges," *to appear in Plasma Sources Sci. Technol.* (1994).

23. S.K. Friedlander, *Smoke, Dust, and Haze,* Wiley, New York, p. 31 (1977).

24. L. Waldmann and K.H. Schmitt, "Thermophoresis and diffusiophoresis of aerosols," *in Aerosol Science*, ed. C.N. Davies, Academic Press, New York (1966).

25. J.E. Daughtery and D.B. Graves, "The role of electrode characteristics in particulate trapping in RF discharges," *10th Symposium on Plasma Processing, ECS,* San Francisco, May (1994).

26. D.J. Rader, A.S. Geller, S.J. Choi, and M.J. Kushner, "Application of numerical models to reduce contamination in semiconductor process environments," *Proc. IES 40th Ann. Tech. Meeting,* 308-315 (1994)

27. G. Evans and R. Greif, "Forced flow near a heated rotating disk: a similarity solutions," *Numerical Heat Transfer 14:* 373-387.

28. D.W. Cooper, R.J. Miller, J.J. Wu, and M.H. Peters, "Deposition of submicron aerosol particles during integrated circuit manufacturing: theory," *Part. Sci. Technol. 8:* 209-224 (1990)

DISCLAIMER